HHS Public Access

Author manuscript

*Ultrasound Med Biol*. Author manuscript; available in PMC 2018 December 01.

Published in final edited form as:

*Ultrasound Med Biol*. 2017 December ; 43(12): 2939–2946. doi:10.1016/j.ultrasmedbio.2017.08.1881.

# A first in human study of acoustic angiography in the breast and peripheral vasculature

**Sarah E. Shelton**[a], **Brooks D. Lindsey**[a], **Paul A. Dayton**[a,b], and **Yueh Z. Lee**[b,c]

[a.] Joint Department of Biomedical Engineering, University of North Carolina-Chapel Hill and North Carolina State University, Raleigh, USA

[b.] Biomedical Research Imaging Center, University of North Carolina-Chapel Hill, USA

[c.] Department of Radiology, University of North Carolina-Chapel Hill, USA

## Abstract

Screening with mammography has been demonstrated to increase breast cancer survival rates by about 20%. However, the current system in which mammography is used to direct patients toward biopsy or surgical excision also results in relatively high rates of unnecessary biopsy, as 66.8% of biopsies are benign. A non-ionizing radiation imaging approach with increased specificity might reduce the rate of unnecessary biopsies. Quantifying the vascular characteristics within and surrounding lesions represents one potential target for assessing likelihood of malignancy via imaging. In this clinical report, we describe the translation of a contrast-enhanced ultrasound technique, acoustic angiography, to human imaging. We demonstrate the feasibility of this technique with initial studies in imaging the hand, wrist, and breast using Definity® microbubble contrast agent and a mechanically-steered prototype dual-frequency transducer in healthy volunteers. Finally, this approach was used to image pre-biopsy BI-RADS 4–5 lesions <2 cm in depth in 11 patients. Results indicate that sensitivity and spatial resolution are sufficient to image vessels as small as 0.2 mm in diameter at depths of ~15 mm in the human breast. Challenges observed include motion artifacts, as well as limited depth of field and sensitivity, which could be improved by correction algorithms and improved transducer technologies.

### Keywords

contrast enhanced ultrasound; breast imaging; angiography; superharmonic; microbubble; microvasculature; dual-frequency

## Introduction

Nearly 250,000 women were diagnosed with breast cancer in the United States in 2016, with over 40,000 deaths in the same year (Howlader 2016). Currently, mammography is used to screen women over the age of 40 and has been shown to increase survival by about 20% (Alexander, et al. 1999, Bjurstam, et al. 2003). Based on mammographic results, the lesion is

corresponding author: Paul A. Dayton, CB 7575, UNC Chapel Hill, Chapel Hill, NC, 27599, padayton@email.unc.edu, (919) 843 9521.

assigned a score from 1 to 6 according to the Breast Imaging Reporting and Data System (BI-RADS) (Radiology 2013). For individuals with a suspicious mammogram (BI-RADS category 3–5), follow-up imaging with other approaches, including diagnostic mammography, breast tomosynthesis (Rafferty, et al. 2013, Shan, et al. 2015, Tucker, et al. 2014), magnetic resonance imaging (Elsamaloty, et al. 2009, Mountford, et al. 2009), and ultrasound (Moon, et al. 2002), may be utilized to clarify the nature of the lesion. Lesions ultimately categorized as BI-RADS 4–5 have a high likelihood of malignancy and are directed toward biopsy or surgical excision.

Pathology results from more than 26,000 patients receiving breast biopsy indicate that 66.8 % of the biopsies were benign, suggesting that many of these biopsies are unnecessary (Weaver, et al. 2006). In addition, breast biopsies are known to yield false negatives at a rate of about 2% (Boba, et al. 2011), and many patients are subjected to repeated biopsies depending primarily on the physician's judgment (Shachar, et al. 2016). About 10% of lesions require repeat biopsy, and only approximately 17% of these are malignant (Youk, et al. 2007), suggesting many patients may be subjected to multiple unnecessary biopsies. If a non-invasive, non-ionizing radiation imaging approach could demonstrate sufficient specificity, it might be possible to reduce the rate of unnecessary biopsies, sparing patients pain and anxiety (Hayes Balmadrid, et al. 2015).

In order for solid tumors to grow beyond a certain size (typically ~2 mm), new vessels must form (angiogenesis) (Bergers and Benjamin 2003, Folkman and Shing 1992). In breast lesions in particular, elevated microvessel density is correlated with the occurrence of metastases and thus has been identified as a potential prognostic indicator, as microvessel density in the region of highest neovascularization has been shown to predict overall and relapse-free survival (Weidner, et al. 1992, Weidner, et al. 1991). Several non-invasive imaging techniques have sought to utilize this knowledge for diagnosis, including magnetic resonance imaging (MRI) (Daldrup-Link, et al. 2003), computed tomography (CT) (Boone, et al. 2006), color Doppler ultrasound (Adler, et al. 1990), and conventional contrast-enhanced ultrasound imaging (Barnard, et al. 2008, Forsberg, et al. 2008, Hoyt, et al. 2015, Sridharan, et al. 2015, Wan, et al. 2012). However, none of these approaches have yet demonstrated the ability to improve diagnostic accuracy or reduce the need for biopsy in clinical studies.

From an imaging perspective, a key challenge is the ability to resolve the microvessels formed early in tumor angiogenesis, as the vessels observed in histological evaluation of invasive carcinomas typically have diameters <100 μm (Ottinetti and Sapino 1988). In order to form vascular or "angiographic" images, many imaging techniques utilize exogenous contrast agents to image vascular structures in the breast, i.e. iodine in CT (Boone, et al. 2006), gadolinium in MRI (Rahbar, et al. 2015), and perfluorocarbon-filled microbubbles in contrast-enhanced ultrasound (Hoyt, et al. 2015). Even with the use of contrast agents, the ability to both detect and resolve the microvessels of clinical interest remains challenging, as typical spatial resolutions for clinical imaging systems are ~700 μm for MRI (Pinker, et al. 2014), ~600 μm for CT (Reiner, et al. 2013), and 300–500 μm for conventional ultrasound (Rissanen, et al. 2008). Special small animal imaging systems have demonstrated higher resolutions in all modalities, including as high as 100–200 μm in MRI (Herrmann, et al.

2012, Jansen, et al. 2009), as high as 40 μm in CT (for scan times >50 min) (Starosolski, et al. 2015), and 30–200 μm for high-frequency ultrasound (Foster, et al. 2009, Foster, et al. 2002).

Contrast-enhanced ultrasound (CEUS) imaging has been performed in the breast for tumor characterization and diagnosis. Ricci characterized CEUS enhancement as having equal accuracy as MRI for breast cancer diagnosis in humans (Ricci, et al. 2007). Subsequent studies have described contrast enhancement and wash-out patterns, but contrast enhanced ultrasound imaging is still not routine in the breast (Liu, et al. 2008, Zhao, et al. 2010). Ultrasound molecular imaging also shows promise as a clinical indicator of malignancy. Microbubbles targeted to vascular endothelial growth factor receptor (VEGFR2) have been validated in model systems (Bzyl, et al. 2013, Pochon, et al. 2010), and it was recently shown in humans that higher targeting was observed in malignant lesions than in benign, and that targeting intensity was related to the level of VEGFR2 expression as measured with immunohistochemistry (Willmann, et al. 2017).

We have recently developed a new contrast-enhanced ultrasound microvascular imaging approach based on the superharmonic signal produced by microbubbles. In this approach microbubbles are excited using a low frequency (<6 MHz) pulse and images are formed from high frequency (>20 MHz) signals produced by microbubbles. Resulting images have higher contrast-to-tissue ratio (CTR, ~25 dB) and spatial resolution (100–200 μm) than conventional contrast-enhanced ultrasound (Lindsey, et al. 2014). Because these images show vascular structures alone, we call this technique acoustic angiography due to the similarity to other forms of angiographic imaging, i.e. computed tomography angiography, magnetic resonance angiography (Rubin and Rofsky 2009). In addition, these images can be segmented and vessel tortuosity computed using previously-established quantitative metrics (Bullitt, et al. 2003, Bullitt, et al. 2006). This is potentially useful because previous studies using intravital microscopy in animal models have shown that tumor vascular remodeling occurs when tumors consist of <100 cells (Li, et al. 2000), providing another potential quantitative metric beyond microvessel density. In imaging a genetically-engineered mouse model of ductal carcinoma, quantifying vessel tortuosity has enabled distinguishing 2–3 mm tumors from healthy tissue (Shelton, et al. 2015).

In this work, we present the first translation of acoustic angiography imaging to humans. Imaging volumes have been acquired of the vasculature in the wrist of healthy volunteers, as well as in the breast of both healthy volunteers and patients. Due to the high spatial resolution of this technique—comparable to that of small animal CT and MRI—it represents a potential tool for quantifying the high microvascular density associated with invasive tumors in the breast. Contrast-enhanced ultrasound imaging utilizing the superharmonic response of microbubbles has been described in *in vitro* and *in vivo* studies, but clinical studies in humans are limited, and were restricted to examinations of the heart at low frequencies (0.8/2.8 MHz) (Bouakaz, et al. 2003). While CEUS allows imaging of tissue perfusion and power Doppler allows imaging of individual vessels at these spatial scales, acoustic angiography reveals vascular morphology and enables quantification of vessel tortuosity, a marker of malignancy.

## Methods

This study was approved by the Institutional Review Board (IRB) of the University of North Carolina at Chapel Hill, and all participants were enrolled after voluntary written informed consent. In the first phase of the study, we enrolled healthy male and female volunteers for initial imaging in the wrist, hand, and breast. Images from these subjects were used to assess the feasibility of superharmonic contrast imaging *in vivo* and determine achievable resolution. A total of 6 individuals volunteered for wrist and hand imaging (3 males, 3 females), and 6 females volunteered for breast imaging. The second phase of the study included a patient population of women with suspicious breast lesions (BI-RADS 4 and 5) who were scheduled to receive a breast biopsy at UNC Hospital. To date, 11 pre-biopsy patients have been imaged in this trial, with enrollment ongoing.

Ten healthy volunteers received an intravenous bolus of 10 μL/kg of Definity (Lantheus Medical Imaging, Billerica, MA) followed by sterile saline, in accordance with the prescribing information, and 2 volunteers received 20 μL/kg. Pre-biopsy participants also received a bolus of Definity at either 10 μL/kg (n=6) or 20 μL/kg (n=5).

Imaging was performed with a VisualSonics Vevo 770 ultrasound scanner and a modified RMV707 transducer (FUJIFILM VisualSonics Inc., Toronto, ON, Canada). The modified transducer has an additional annular low frequency element (4 MHz center frequency) confocal to the 707 transducer (30 MHz center frequency) in order to allow dual-frequency imaging of microbubble superharmonics by transmitting with the low frequency element and receiving with the high frequency element (Gessner, et al. 2010). Dual-frequency imaging was conducted at a mechanical index of 0.6 (non-derated), which is within the range suggested for safe use with Definity (up to 0.8).

Three-dimensional image volumes were acquired using a linear motion stage, which translated the transducer across the surface of the skin with a step size of 0.2 mm. This motion stage (FUJIFILM VisualSonics Inc., Toronto, ON, Canada) was designed to operate fixed to a platform for small animal imaging, so to enable more flexible positioning for human patients, we mounted the motion stage to an adjustable arm (Photo Variable Friction Arm, Manfrotto, South Upper Saddle River, NJ), supported by a surgical microscope stand. Each image slice in a 3D volume was acquired at a rate of 3 frames per second, with a 3D volume being acquired in approximately 1–2 minutes, depending on the length of the scan (20–30 mm). The transducer (attached to the motion stage) was positioned by a radiologist and then locked into place to acquire 3-D scans.

De-identified image data was exported for offline analysis and image reconstruction in ImageJ and the VisualSonics Vevo770 imaging software. Volumetric data sets were rendered using maximum intensity projections to display 3-D images in 2-D. Linear interpolation was used to compensate for larger spacing in the elevation direction than the axial-lateral dimension when reconstructing images in orientations other than the acquisition plane.

## Results

This study has demonstrated the feasibility of superharmonic acoustic angiography in human subjects for the first time. We were able to visualize contrast signal and resolve individual vessels using the standard clinical dose of Definity microbubbles, 10 μL/kg. Additionally, we also tested twice the standard dose of Definity, 20 μL/kg, in 5 patients and 2 healthy volunteers and observed stronger contrast signal at the higher dose. Figure 1 shows examples of acquired images of the wrists of 2 different healthy volunteers. These images are maximum intensity projections of the 3-D image volumes and show the radial artery and the branch of the smaller palmar radiocarpal artery. Both images were acquired immediately following a bolus of 10 μL/kg of contrast. On the left (1A), an extent of approximately 2.5 cm of the radial artery is shown, while the image on the right (1B) is enlarged to show detail from a different subject. The diameters of the radial arteries visible in these images was measured to be between 1.5 and 2 mm wide, consistent with the range observed in other measurements of radial artery size (Kotowycz, et al. 2014).

The images in Figure 2 were acquired in healthy volunteers and show several branching structures and vasculature of different sizes in normal breast tissue. Both of these subjects received the 10 μL/kg contrast dose. Additionally, these images also reveal one of the limitations of the confocal, single-element transducer design: the limited depth of field. The transducer elements are focused at a depth of 1.3 cm, and the high frequency element has a depth of field of 2.2 mm, as reported by the manufacturer. In practice, these images show that region of tissue where contrast is visible in dual-frequency imaging spans approximately 8 mm, centered at the focus. In Figure 2A, the vessels seem to drop off as they plunge deeper into the tissue, and in 2B, the deep vessel that crosses the center of the image has a weaker signal than the nearby vessels despite the fact that they are similar in size.

Figure 3 shows a maximum intensity projection with several vessel diameters measured and annotated on the image. This image is the same data as seen in Figure 2B, reconstructed with a maximum intensity projection at a slightly different angle. In Figure 3, we see small vessels measuring 0.17 mm wide, with low image contrast. However, slightly larger 0.2 mm vessels have higher contrast, with the largest vessels between 0.43 and 1.24 mm being the easiest to visualize.

While the maximum intensity projections of the 3-D data are useful for resolving the structure of vascular morphology throughout the tissue, there is additional information available in individual image frames. Figure 4 includes images from a pre-biopsy patient who received 20 μL/kg of Definity. Figure 4A is a maximum intensity projection showing large vessels branching as well as diffuse contrast signal from sub-resolution vasculature in the surrounding tissue. Figure 4B is an enlarged view of the main branch, also shown as a maximum intensity projection. Figure 4C, however, is a single frame from the branching region showing that multiple small vessels are resolvable in the individual frame, but less apparent in the projected data. Therefore, individual frames of acoustic angiography images could be used to understand the relative positions and connections between sub-millimeter vessels.

Comparing the breast images shown in Figure 5 to the wrist images in Figure 1, we can see more artifact due to respiration in Figure 5. The borders of the vessels in Figure 5 are less smooth than those seen in Figure 1 due to tissue motion. However, in these examples, respiration motion on the order of 0.3 to 0.5 mm (Figure 4B, Figure 5B) is not large enough to obscure the overall morphology. Additionally, we can perform motion correction by applying B-spline registration to consecutive frames in the image to produce smoothed images without altering the overall vessel morphology, a demonstrated in figure 6.

No serious adverse reactions to the contrast occurred. However, four participants reported mild events. One participant (out of 16) who received 10 μL/kg reported transient back and chest discomfort, and 3 participants (out of 7) who received a bolus of 20 μL/kg experienced mild, transient flushing with no significant changes in vital signs. Although these mild reactions were anticipated in the package insert for Definity, the incidence was higher than expected in our small sample size. It is unknown if this might have been due to an issue with the contrast agent lot, the bolus administration rate, a random occurrence in our patient population, or some other variable. It is worth noting that other groups have used the same contrast agent at the same dose without any reported adverse reactions (Sridharan, et al. 2005). As the acoustic angiography imaging approach uses standard clinical imaging parameters (4 MHz, MI = 0.6), it seems unlikely that observed adverse reactions were related to the imaging technique itself.

## Discussion

In this study, we only included lesions located within approximately 1.5 cm from the skin surface due to the limited depth of field provided by the fixed focus transducer. This prototype, confocal, single-element transducer has a lens with a fixed focus of 13 mm and an approximate field of view of 8 mm in dual-frequency contrast imaging mode. Both the field of view and frame rate might be improved by the development of a dual-frequency array. With a higher frame rate enabled by acquiring an entire imaging slice in real-time without mechanically sweeping the confocally-aligned transducer elements, motion artifacts could be minimized by acquiring the entire 3D image in single breath-hold (~10 sec) using a translation stage. There is also a clinical need to image lesions deeper than 1.5 cm. Though it is estimated that 30% of breast lesions are located within 1 cm of the skin surface, a larger imaging depth will be necessary to make superharmonic contrast imaging feasible relevant to a greater number of patients (Feig, et al. 1977). Acoustic angiography can be performed with greater depth of penetration by selecting a lower receive frequency, and we have demonstrated superharmonic contrast imaging as deep as 4 cm using an endoscopic transducer designed to transmit at 4 MHz and receive at 20 MHz (Lindsey, et al. 2017). Axial resolution at this frequency combination is expected to be better than 200 μm (Lindsey, et al. 2014).

Of note, the sensitivity and spatial resolution of the current system used in this study allowed acquisition of images with vessels as small as 100–200 μm (Figure 3), similar to the resolution provided by pre-clinical MRI and CT systems (Herrmann, et al. 2012, Jansen, et al. 2009, Starosolski, et al. 2015). Improvements in sensitivity would require either improved transducer sensitivity or increased microbubble dose.

Super-resolution imaging techniques have demonstrated resolution below the diffraction limit, nearly at the capillary scale, using microbubble localization techniques (Christensen-Jeffries, et al. 2015, Desailly, et al. 2013, Errico, et al. 2015, Lin, et al. 2017, O'Reilly and Hynynen 2013, Viessmann, et al. 2013). However, super-resolution imaging has not yet been demonstrated in the clinic and requires the acquisition of thousands to tens of thousands of images to create a single frame. Even with ultrafast plane-wave imaging, the acquisition time for a single frame is on the order of minutes in order to accumulate a sufficient number of microbubble positions to reconstruct microvascular structure with fine detail. Though superharmonic acoustic angiography cannot match the resolution scale promised by super-resolution imaging, microvessels approximately 100–200 μm can be imaged with a single transmit event, and a 3D image volume can be acquired in 1–2 minutes using a translation stage. Dual-frequency array transducers are expected to significantly improve acquisition time for acoustic angiography in the future.

Improving spatial resolution would require either a larger aperture (which would likely prove increasingly difficult to couple to the patient), or the use of a higher receiving frequency. Unfortunately, increasing the receiving frequency would result in a decrease in sensitivity, as the superharmonic signals used to form these images decrease in amplitude with increasing frequency (Lindsey, et al. 2014), in addition to increasing attenuation, which would also decrease the depth of penetration. Nonetheless, if this technology could be utilized in conjunction with breast ultrasound, existing resolution and sensitivity may eventually prove sufficient for a diagnostic test with adequate specificity to preclude biopsy in lesions lacking vessels greater than approximately 150 μm in diameter. It is worth noting that this technology has demonstrated potential for use for imaging other shallow vasculature such as the carotid arteries for assessment of atherosclerotic disease.

## Acknowledgements

Funding was provided by the National Institute of Health from R01CA170665S1, R01CA170665, F99CA212227, and F32EB018715. We would also like to acknowledge the contributions of Michele Vickers, Shanah Kirk, Terry Hartman, nursing support from the UNC Clinical and Translational Research Center, and the cooperation of the physicians and staff of the Breast Imaging Division in the Department of Radiology. We also thank Samuel Gerber and Stephen Aylward (Kitware, Inc.) for their expert help with image registration. This imaging would not have been possible without the collaborative efforts of Dr. F. Stuart Foster, Mike Lee, Emmanuel Cherin, Chris Chaggares, and technical support from Visualsonics, Inc. P.A.D. declares that he is an inventor on a patent describing the dual-frequency imaging technology, and is a co-founder of SonoVol, Inc., a company which has licensed this technology.

## References

Adler DD, Carson PL, Rubin JM, Quinn-Reid D. Doppler ultrasound color flow imaging in the study of breast cancer: preliminary findings. Ultrasound Med Biol 1990; 16:553–9. [PubMed: 2238263]

Alexander FE, Anderson TJ, Brown HK, Forrest AP, Hepburn W, Kirkpatrick AE, Muir BB, Prescott RJ, Smith A. 14 years of follow-up from the Edinburgh randomised trial of breast-cancer screening. Lancet 1999; 353:1903–8. [PubMed: 10371567]

Barnard S, Leen E, Cooke T, Angerson W. A contrast-enhanced ultrasound study of benign and malignant breast tissue. South African medical journal = Suid-Afrikaanse tydskrif vir geneeskunde 2008; 98:386–91. [PubMed: 18637311]

Bergers G, Benjamin LE. Tumorigenesis and the angiogenic switch. Nature reviews. Cancer 2003; 3:401–10. [PubMed: 12778130]

Bjurstam N, Bjorneld L, Warwick J, Sala E, Duffy SW, Nystrom L, Walker N, Cahlin E, Eriksson O, Hafstrom LO, Lingaas H, Mattsson J, Persson S, Rudenstam CM, Salander H, Save-Soderbergh J, Wahlin T. The Gothenburg Breast Screening Trial. Cancer 2003; 97:2387–96. [PubMed: 12733136]

Boba M, Koltun U, Bobek-Billewicz B, Chmielik E, Eksner B, Olejnik T. False-negative results of breast core needle biopsies - retrospective analysis of 988 biopsies. Polish journal of radiology 2011; 76:25–9.

Boone JM, Kwan AL, Yang K, Burkett GW, Lindfors KK, Nelson TR. Computed tomography for imaging the breast. Journal of mammary gland biology and neoplasia 2006; 11:103–11. [PubMed: 17053979]

Bouakaz A, Krenning BJ, Vletter WB, ten Cate FJ, De Jong N. Contrast superharmonic imaging: a feasibility study. Ultrasound Med Biol 2003; 29:547–53. [PubMed: 12749924]

Bullitt E, Gerig G, Pizer SM, Lin W, Aylward SR. Measuring tortuosity of the intracerebral vasculature from MRA images. IEEE transactions on medical imaging 2003; 22:1163–71. [PubMed: 12956271]

Bullitt E, Wolthusen PA, Brubaker L, Lin W, Zeng D, Van Dyke T. Malignancy-associated vessel tortuosity: a computer-assisted, MR angiographic study of choroid plexus carcinoma in genetically engineered mice. AJNR. American journal of neuroradiology 2006; 27:612–9. [PubMed: 16552004]

Bzyl J, Palmowski M, Rix A, Arns S, Hyvelin J-M, Pochon S, Ehling J, Schrading S, Kiessling F, Lederle W. The high angiogenic activity in very early breast cancer enables reliable imaging with VEGFR2-targeted microbubbles (BR55). Eur Radiol 2013; 23:468–75. [PubMed: 22878592]

Christensen-Jeffries K, Browning RJ, Tang MX, Dunsby C, Eckersley RJ. In vivo acoustic super-resolution and super-resolved velocity mapping using microbubbles. IEEE transactions on medical imaging 2015; 34:433–40. [PubMed: 25265604]

Daldrup-Link HE, Rydland J, Helbich TH, Bjornerud A, Turetschek K, Kvistad KA, Kaindl E, Link TM, Staudacher K, Shames D, Brasch RC, Haraldseth O, Rummeny EJ. Quantification of breast tumor microvascular permeability with feruglose-enhanced MR imaging: initial phase II multicenter trial. Radiology 2003; 229:885–92. [PubMed: 14576446]

Desailly Y, Couture O, Fink M, Tanter M. Sono-activated ultrasound localization microscopy. Appl Phys Lett 2013; 103.

Elsamaloty H, Elzawawi MS, Mohammad S, Herial N. Increasing accuracy of detection of breast cancer with 3-T MRI. AJR. American journal of roentgenology 2009; 192:1142–8. [PubMed: 19304726]

Errico C, Pierre J, Pezet S, Desailly Y, Lenkei Z, Couture O, Tanter M. Ultrafast ultrasound localization microscopy for deep super-resolution vascular imaging. Nature 2015; 527:499–502. [PubMed: 26607546]

Feig SA, Shaber GS, Patchefsky A, Schwartz GF, Edeiken J, Libshitz HI, Nerlinger R, Curley RF, Wallace JD. Analysis of clinically occult and mammographically occult breast tumors. AJR. American journal of roentgenology 1977; 128:403–8. [PubMed: 190908]

Folkman J, Shing Y. Angiogenesis. The Journal of biological chemistry 1992; 267:10931–4. [PubMed: 1375931]

Forsberg F, Kuruvilla B, Pascua MB, Chaudhari MH, Merton DA, Palazzo JP, Goldberg BB. Comparing contrast-enhanced color flow imaging and pathological measures of breast lesion vascularity. Ultrasound Med Biol 2008; 34:1365–72. [PubMed: 18436369]

Foster FS, Mehi J, Lukacs M, Hirson D, White C, Chaggares C, Needles A. A new 15–50 MHz array-based micro-ultrasound scanner for preclinical imaging. Ultrasound Med Biol 2009; 35:1700–8. [PubMed: 19647922]

Foster FS, Zhang MY, Zhou YQ, Liu G, Mehi J, Cherin E, Harasiewicz KA, Starkoski BG, Zan L, Knapik DA, Adamson SL. A new ultrasound instrument for in vivo microimaging of mice. Ultrasound Med Biol 2002; 28:1165–72. [PubMed: 12401387]

Gessner R, Lukacs M, Lee M, Cherin E, Foster FS, Dayton PA. High-resolution, high-contrast ultrasound imaging using a prototype dual-frequency transducer: in vitro and in vivo studies. IEEE transactions on ultrasonics, ferroelectrics, and frequency control 2010; 57:1772–81.

Hayes Balmadrid MA, Shelby RA, Wren AA, Miller LS, Yoon SC, Baker JA, Wildermann LA, Soo MS. Anxiety prior to breast biopsy: Relationships with length of time from breast biopsy recommendation to biopsy procedure and psychosocial factors. Journal of health psychology 2015.

Herrmann KH, Schmidt S, Kretz A, Haenold R, Krumbein I, Metzler M, Gaser C, Witte OW, Reichenbach JR. Possibilities and limitations for high resolution small animal MRI on a clinical whole-body 3T scanner. Magma 2012; 25:233–44. [PubMed: 22042538]

Howlader NNA, Krapcho M, Garshell J, Neyman N, Altekruse SF, Kosary CL, Yu M, Ruhl J, Tatalovich Z, Cho H, Mariotto A, Lewis DR, Chen HS, Feuer EJ, Cronin KA (eds.). 2016 SEER Cancer Statistics Review, 1973–2013. Bethesda, MD: National Cancer Institute.

Hoyt K, Umphrey H, Lockhart M, Robbin M, Forero-Torres A. Ultrasound imaging of breast tumor perfusion and neovascular morphology. Ultrasound Med Biol 2015; 41:2292–302. [PubMed: 26116159]

Jansen SA, Paunesku T, Fan XB, Woloschak GE, Vogt S, Conzen SD, Krausz T, Newstead GM, Karczmar GS. Ductal Carcinoma in Situ: X-ray Fluorescence Microscopy and Dynamic Contrast-enhanced MR Imaging Reveals Gadolinium Uptake within Neoplastic Mammary Ducts in a Murine Model. Radiology 2009; 253:399–406. [PubMed: 19864527]

Kotowycz MA, Johnston KW, Ivanov J, Asif N, Almoghairi AM, Choudhury A, Nagy CD, Sibbald M, Chan W, Seidelin PH, Barolet AW, Overgaard CB, Dzavik V. Predictors of radial artery size in patients undergoing cardiac catheterization: insights from the Good Radial Artery Size Prediction (GRASP) study. The Canadian journal of cardiology 2014; 30:211–6. [PubMed: 24461923]

Li CY, Shan S, Huang Q, Braun RD, Lanzen J, Hu K, Lin P, Dewhirst MW. Initial stages of tumor cell-induced angiogenesis: evaluation via skin window chambers in rodent models. Journal of the National Cancer Institute 2000; 92:143–7. [PubMed: 10639516]

Lin F, Shelton SE, Espindola D, Rojas JD, Pinton G, Dayton PA. 3-D Ultrasound Localization Microscopy for Identifying Microvascular Morphology Features of Tumor Angiogenesis at a Resolution Beyond the Diffraction Limit of Conventional Ultrasound. Theranostics 2017; 7:196–204. [PubMed: 28042327]

Lindsey BD, Kim J, Dayton PA, Jiang X. Dual-Frequency Piezoelectric Endoscopic Transducer for Imaging Vascular Invasion in Pancreatic Cancer. IEEE transactions on ultrasonics, ferroelectrics, and frequency control 2017.

Lindsey BD, Rojas JD, Martin KH, Shelton SE, Dayton PA. Acoustic characterization of contrast-to-tissue ratio and axial resolution for dual-frequency contrast-specific acoustic angiography imaging. IEEE transactions on ultrasonics, ferroelectrics, and frequency control 2014; 61:1668–87.

Liu H, Jiang YX, Liu JB, Zhu QL, Sun Q. Evaluation of breast lesions with contrast-enhanced ultrasound using the microvascular imaging technique: Initial observations. Breast 2008; 17:532–39. [PubMed: 18534851]

Moon WK, Noh DY, Im JG. Multifocal, multicentric, and contralateral breast cancers: bilateral whole-breast US in the preoperative evaluation of patients. Radiology 2002; 224:569–76. [PubMed: 12147858]

Mountford C, Ramadan S, Stanwell P, Malycha P. Proton MRS of the breast in the clinical setting. NMR in biomedicine 2009; 22:54–64. [PubMed: 19086012]

O'Reilly MA, Hynynen K. A super-resolution ultrasound method for brain vascular mapping. Med Phys 2013; 40:110701. [PubMed: 24320408]

Ottinetti A, Sapino A. Morphometric Evaluation of Microvessels Surrounding Hyperplastic and Neoplastic Mammary Lesions. Breast cancer research and treatment 1988; 11:241–48. [PubMed: 2458784]

Pinker K, Bogner W, Baltzer P, Trattnig S, Gruber S, Abeyakoon O, Bernathova M, Zaric O, Dubsky P, Bago-Horvath Z, Weber M, Leithner D, Helbich TH. Clinical application of bilateral high temporal and spatial resolution dynamic contrast-enhanced magnetic resonance imaging of the breast at 7 T. European radiology 2014; 24:913–20. [PubMed: 24306425]

Pochon S, Tardy I, Bussat P, Bettinger T, Brochot J, von Wronski M, Passantino L, Schneider M. BR55: a lipopeptide-based VEGFR2-targeted ultrasound contrast agent for molecular imaging of angiogenesis. Invest Radiol 2010; 45:89–95. [PubMed: 20027118]

Radiology ACo. Breast Imaging Reporting and Data System BI-RADS. Reston, VA: American College of Radiology, 2013.

Rafferty EA, Park JM, Philpotts LE, Poplack SP, Sumkin JH, Halpern EF, Niklason LT. Assessing Radiologist Performance Using Combined Digital Mammography and Breast Tomosynthesis Compared with Digital Mammography Alone: Results of a Multicenter, Multireader Trial. Radiology 2013; 266:104–13. [PubMed: 23169790]

Rahbar H, DeMartini WB, Lee AY, Partridge SC, Peacock S, Lehman CD. Accuracy of 3 T versus 1.5 T breast MRI for pre-operative assessment of extent of disease in newly diagnosed DCIS. European journal of radiology 2015; 84:611–6. [PubMed: 25604909]

Reiner CS, Roessle M, Thiesler T, Eberli D, Klotz E, Frauenfelder T, Sulser T, Moch H, Alkadhi H. Computed tomography perfusion imaging of renal cell carcinoma: systematic comparison with histopathological angiogenic and prognostic markers. Investigative radiology 2013; 48:183–91. [PubMed: 23328912]

Ricci P, Cantisani V, Ballesio L, Pagliara E, Sallusti E, Drudi FM, Trippa F, Calascibetta F, Erturk SM, Modesti M, Passariello R. Benign and malignant breast lesions: efficacy of real time contrast-enhanced ultrasound vs. magnetic resonance imaging. Ultraschall in der Medizin 2007; 28:57–62. [PubMed: 17304413]

Rissanen TT, Korpisalo P, Karvinen H, Liimatainen T, Laidinen S, Grohn OH, Yla-Herttuala S. High-resolution ultrasound perfusion imaging of therapeutic angiogenesis. JACC. Cardiovascular imaging 2008; 1:83–91. [PubMed: 19356410]

Rubin GD, Rofsky NM. CT and MR Angiography: Comprehensive Vascular Assessment. Philadelphia: Lippincott Williams & Wilkins, 2009.

Shachar SS, Fried G, Drumea K, Shafran N, Bar-Sela G. Physicians' Considerations for Repeat Biopsy in Patients With Recurrent Metastatic Breast Cancer. Clinical breast cancer 2016; 16:e43–8. [PubMed: 26642811]

Shan J, Tucker AW, Lee YZ, Heath MD, Wang XH, Foos DH, Lu JP, Zhou O. Stationary chest tomosynthesis using a carbon nanotube x-ray source array: a feasibility study. Physics in medicine and biology 2015; 60:81–100. [PubMed: 25478786]

Shelton SE, Lee YZ, Foster FS, Lee M, Cherin E, Aylward SR, Dayton PA. Quantification of microvascular tortuosity during tumor evolution utilizing acoustic angiography. Ultrasound Med Biol 2015; 41:1896–904. [PubMed: 25858001]

Sridharan A, Eisenbrey JR, Machado P, Ojeda-Fournier H, Wilkes A, Sevrukov A, Mattrey RF, Wallace K, Chalek CL, Thomenius KE, Forsberg F. Quantitative Analysis of Vascular Heterogeneity in Breast Lesions Using Contrast-Enhanced 3-D Harmonic and Subharmonic Ultrasound Imaging. Ieee T Ultrason Ferr 2015; 62:502–10.

Starosolski Z, Villamizar CA, Rendon D, Paldino MJ, Milewicz DM, Ghaghada KB, Annapragada AV. Ultra High-Resolution In vivo Computed Tomography Imaging of Mouse Cerebrovasculature Using a Long Circulating Blood Pool Contrast Agent. Sci Rep-Uk 2015; 5.

Tucker AW, Calliste J, Gidcumb EM, Wu J, Kuzmiak CM, Hyun N, Zeng DL, Lu JP, Zhou O, Lee YZ. Comparison of a Stationary Digital Breast Tomosynthesis System to Magnified 2D Mammography Using Breast Tissue Specimens. Academic radiology 2014; 21:1547–52. [PubMed: 25172412]

Viessmann OM, Eckersley RJ, Christensen-Jeffries K, Tang MX, Dunsby C. Acoustic super-resolution with ultrasound and microbubbles. Phys Med Biol 2013; 58:6447–58. [PubMed: 23999099]

Wan CF, Du J, Fang H, Li FH, Zhu JS, Liu Q. Enhancement patterns and parameters of breast cancers at contrast-enhanced US: correlation with prognostic factors. Radiology 2012; 262:450–9. [PubMed: 22282183]

Weaver DL, Rosenberg RD, Barlow WE, Ichikawa L, Carney PA, Kerlikowske K, Buist DS, Geller BM, Key CR, Maygarden SJ, Ballard-Barbash R. Pathologic findings from the Breast Cancer Surveillance Consortium: population-based outcomes in women undergoing biopsy after screening mammography. Cancer 2006; 106:732–42. [PubMed: 16411214]

Weidner N, Folkman J, Pozza F, Bevilacqua P, Allred EN, Moore DH, Meli S, Gasparini G. Tumor angiogenesis: a new significant and independent prognostic indicator in early-stage breast carcinoma. Journal of the National Cancer Institute 1992; 84:1875–87. [PubMed: 1281237]

Weidner N, Semple JP, Welch WR, Folkman J. Tumor angiogenesis and metastasis--correlation in invasive breast carcinoma. The New England journal of medicine 1991; 324:1–8.

Willmann JK, Bonomo L, Carla Testa A, Rinaldi P, Rindi G, Valluru KS, Petrone G, Martini M, Lutz AM, Gambhir SS. Ultrasound Molecular Imaging With BR55 in Patients With Breast and Ovarian Lesions: First-in-Human Results. Journal of Clinical Oncology 2017:JCO.2016708594.

Youk JH, Kim EK, Kim MJ, Lee JY, Oh KK. Missed breast cancers at US-guided core needle biopsy: How to reduce them. Radiographics 2007; 27:79–U9. [PubMed: 17235000]

Zhao H, Xu R, Ouyang Q, Chen L, Dong B, Huihua Y. Contrast-enhanced ultrasound is helpful in the differentiation of malignant and benign breast lesions. European Journal of Radiology 2010; 73:288–93. [PubMed: 19559551]

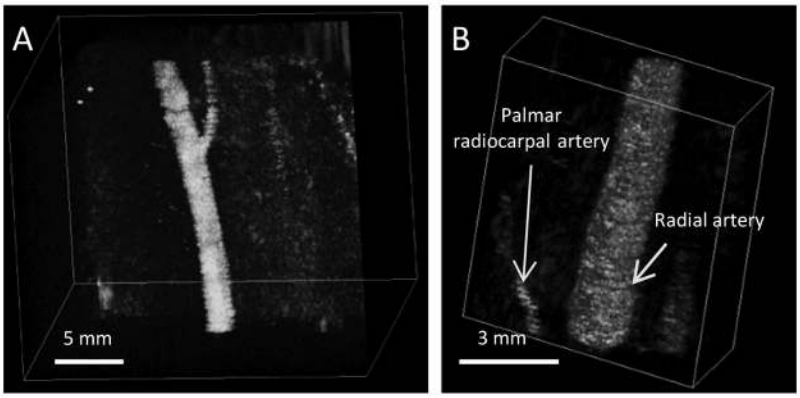


**Figure 1.**

Maximum intensity projections of acoustic angiography images acquired in the wrists of volunteers administered a bolus of 10 μL/kg of Definity®.

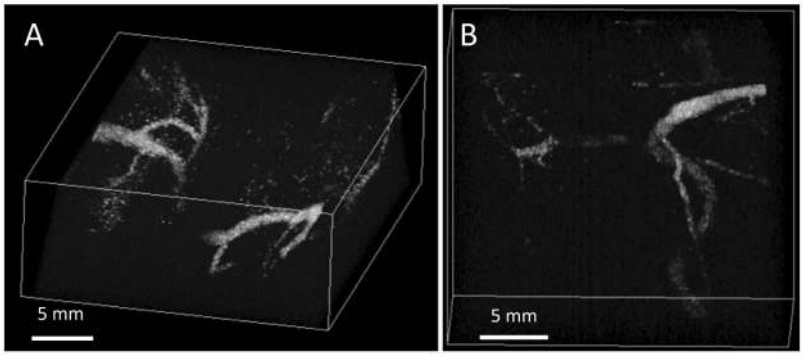


**Figure 2.**
Images of normal breast vasculature in healthy volunteers who received a 10 μL/kg bolus.

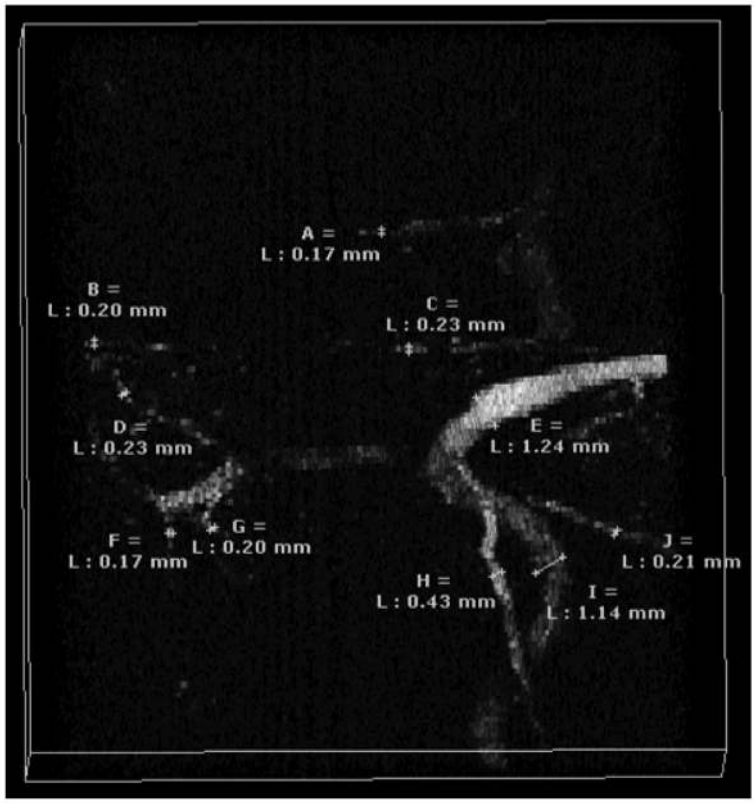


**Figure 3.**

A maximum intensity projection of breast vasculature from a healthy volunteer annotated with vessel diameters.

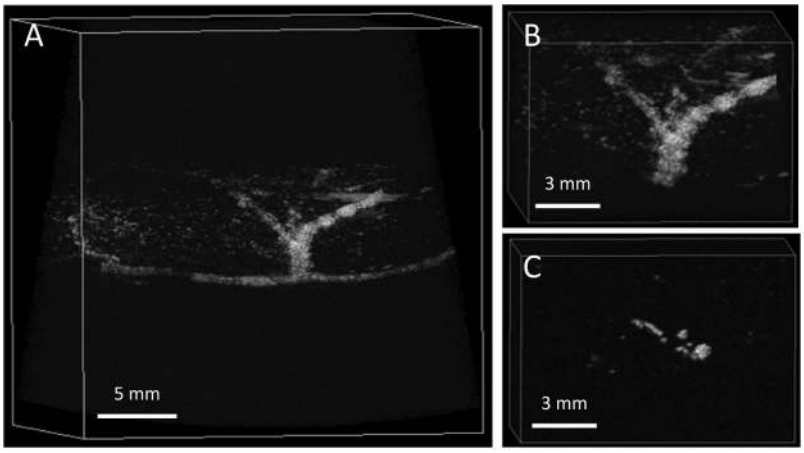


**Figure 4.**

Images from a pre-biopsy patient who received a bolus of 20 μL/kg of contrast. 4A shows a maximum intensity projection of the image volume, while 4B is enlarged to show detail at the main branching location. 4C is a single frame at the same scale as 4B, showing several distinct vessels in the branching region.

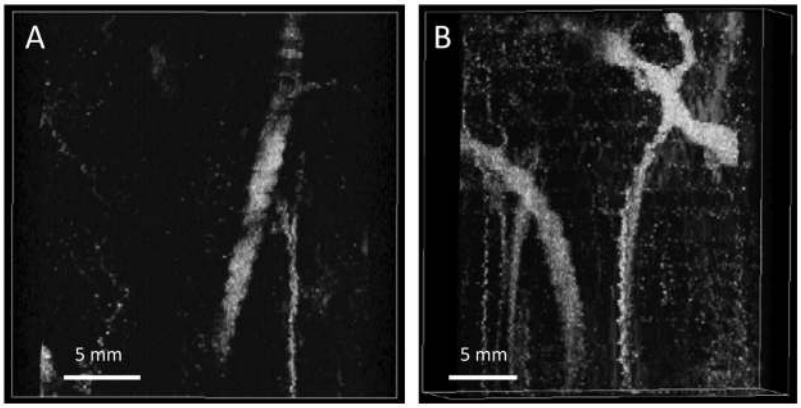


**Figure 5.**

Images from pre-biopsy patients showing vasculature ranging in size from approximately 0.2 to 2 mm in diameter. Respiration motion artifacts are visible, making the borders of the vessels appear serrated. Subjects received 10 μL/kg of Definity.

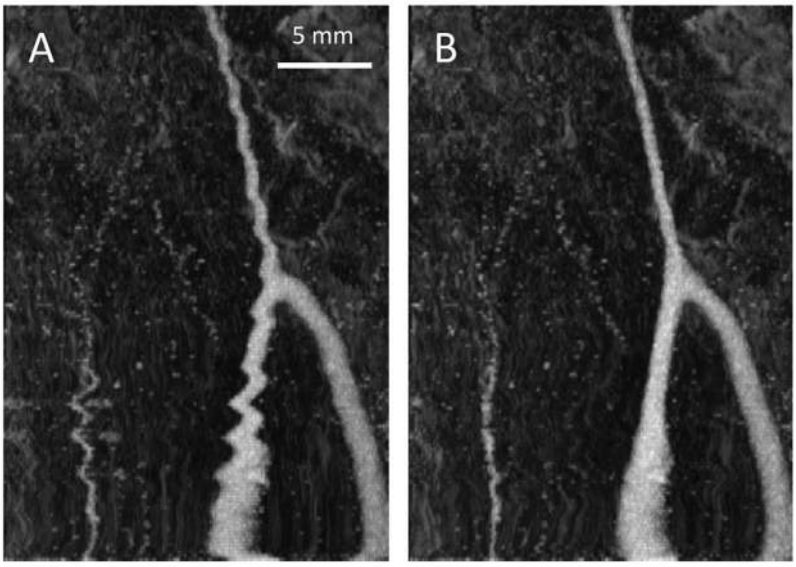


**Figure 6.**

Image from a pre-biopsy patient who received 10 μL/kg of Definity. 6A shows the original image, clearly subject to respiration motion. 6B shows the motion corrected image using B-spline registration.